The Interaction Between Electrogalvanized Zinc Deposit Structure and the Forming Properties of Sheet Steel

By J.H. Lindsay, R.F. Paluch, H.D. Nine, V.R. Miller and T.J. O'Keefe

The use of electrogalvanized steel to enhance the corrosion resistance of automobile body panels affects the forming of sheet steel. The zinc structure and morphology, influenced by electrolytic and hydrodynamic conditions during deposition, alters the drawing character of the sheet. Steel plated with zinc deposits exhibiting strong basal (0001) plane and strong pyramid plane (10$\bar{1}$X) orientation were prepared. Forming properties were related to deposit morphology and structure and compared to those for commercial products.

The automotive industry uses electrogalvanized steel sheet to increase the corrosion resistance of body panels. This material meets standards of 5-years' resistance to "cosmetic" deterioration and 10-years' resistance to basis metal perforation. During manufacture, the sheet is blanked, formed, spot welded, phosphated, and painted. While its main purpose is to enhance corrosion resistance via sacrificial protection, the coating must not hamper subsequent operations. The success of industrial electrogalvanizing requires a deposit structure compatible with these processes. This paper considers the interaction between the zinc deposit structure and formability.

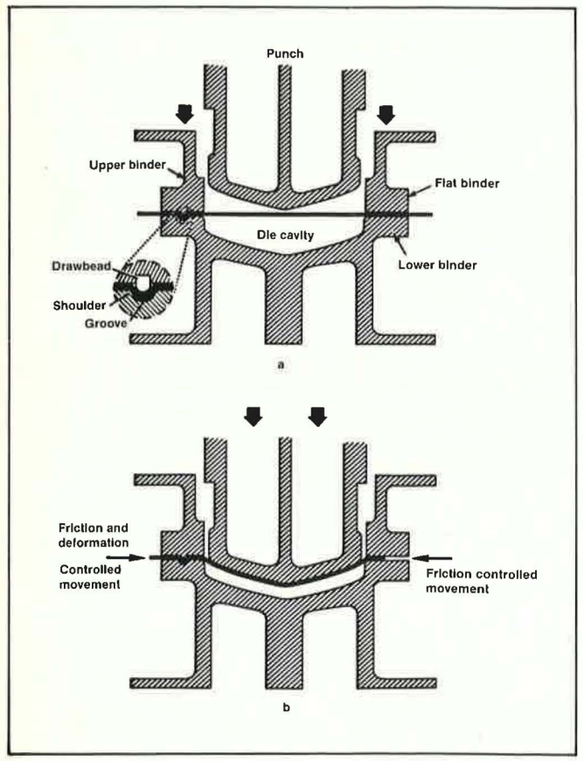

Fig. 1—Double action press used in sheet metal stamping. (a) Upper binder moves down to hold the sheet metal in position for forming (inset shows drawbead geometry); (b) punch moves down into lower die cavity, drawing the sheet metal into the die through the binders.

Sheet Metal Forming

In stamping, a double-action press is used. As shown in Fig. 1, the upper die half contains the upper binder and the punch. These are complemented in the lower half by the lower binder and die cavity, respectively. As the die is closed, the upper binder descends on the outer rim of the sheet metal blank to hold it in place (Fig. 1a). The punch then moves downward to form the metal (Fig. 1b).

During forming, metal is drawn from the binder into the cavity. The binder surface controls the metal flow. The restraining force must be high enough to prevent excessive flow, which causes wrinkling, and yet low enough to avoid tearing. The right side of Fig. 1a shows a flat binder, where

Fig. 2—SEM photograph of the surface of a typical commercial electrogalvanized zinc coating.

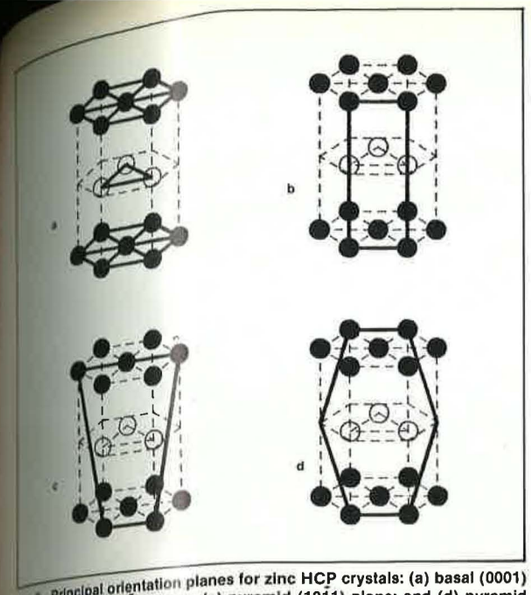

Fig. 3—Principal orientation planes for zinc HCP crystals: (a) basal (0001) plane; (b) prism (10$\bar{1}$0) plane; (c) pyramid (10$\bar{1}$1) plane; and (d) pyramid (10$\bar{1}$2) plane.

frictional forces are the sole means of restraint. This is often insufficient to retard metal flow. A drawbead, shown on the left side of Fig. 1a, offers more restraint by adding a deformation component.[1] With drawbeads, deformation provides 75 percent of the restraining force, friction provides the remainder.[1,2]

Drawbeads are also used in metal forming research. Studies of the friction and deformation components of drawbead forces have been used to model forming processes.[3] Such work has shed light on the effects of material, lubricant, and surface conditions on drawing characteristics.[1-4] The use of coated metals presents another variable. Work on hot-dipped and electrogalvanized products has shown that the coating can affect forming.[3-5] Correlations between surface morphology and friction have been suggested.[4]

Zinc Structure and Surface Morphology

Commercial electrogalvanized coatings are fine-grained and have a surface such as that shown in Fig. 2. The main feature is a predominance of hexagonal platelets, 5 to 10 μm in size, whose hexagonal faces are tilted with respect to the sheet plane. This morphology differs from that of bare cold-rolled sheet steel, where a directional pattern of rolling marks is normally seen.

Referring to the hexagonal close-packed (HCP) lattice in Fig. 3, the hexagonal faces correspond to the basal (0001) planes (Fig. 3a). Deposits with basal planes lying parallel to the substrate are not obtained commercially. This also holds for basal planes perpendicular to the substrate, where a prism plane [e.g., (10$\bar{1}$0), Fig. 3b] is aligned with the surface. Rather, commercial deposits fall between these two limits. In the sample shown in Fig. 2, the pyramid planes [e.g., (10$\bar{1}$1), (10$\bar{1}$2), Fig. 3c,d] parallel the substrate. X-ray diffraction shows a strong pyramidal orientation. A preponderance of high index planes (10$\bar{1}$3+) would result in the basal planes being tilted at a shallow angle. With the low index, (10$\bar{1}$1) and (10$\bar{1}$2) planes dominant, the platelets would be tilted at a steeper angle.

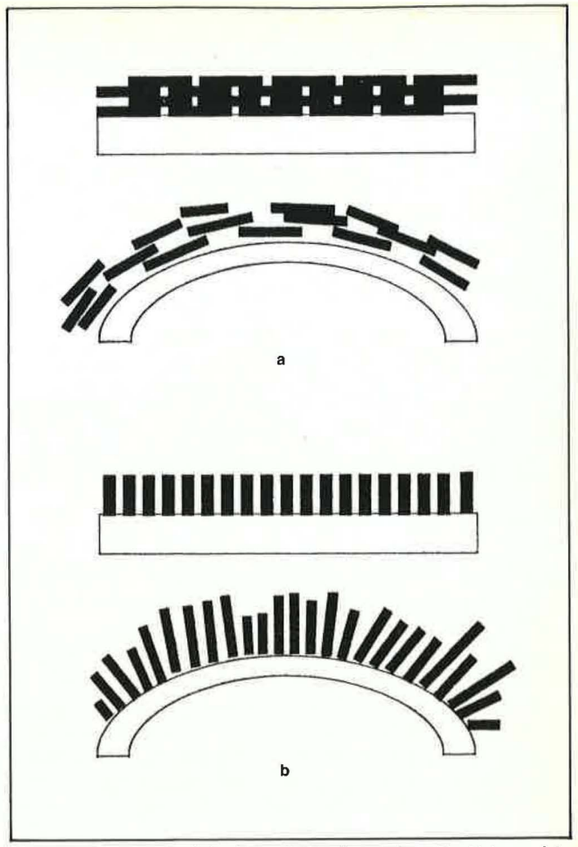

Fig. 4—Consequences of simple tensile bending on deposits of (a) complete basal (0001) and (b) prism (10$\bar{1}$0) plane orientation.

Earlier work[6-8] has shown that structure and morphology can be controlled with specific values of temperature, pH, flow rate, and current density.[6] A strong basal (0001) orientation was produced at low pH (1.5) in a sulfate electrolyte (150 g/L Zn). No deposits were obtained with strong prism plane (10$\bar{1}$0) orientation, but deposits with low-index pyramid [(10$\bar{1}$1), (10$\bar{1}$2)] plane alignment were obtained under other conditions.

Zinc Coating Deformation

Plastic deformation in crystalline solids involves slip, the displacement of one atom plane over another by dislocation movement.[9] The slip plane is that with the highest density of atoms within it; for HCP lattices, the major slip plane is the basal (0001) plane.

For the cases of total basal or total prism plane orientation, each should behave differently under deformation, as in Fig. 4. Plastic deformation of basal-plane deposits would elongate individual grains and cause one layer of grains to slide over the next (Fig. 4a). This would preserve continuity, which is essential for corrosion resistance. For prism-plane deposits, the stress is normal to the slip plane and fracture would be likely (Fig. 4b).

In practice, the results are not so simple. The stamping section in Fig. 5 is deformed by convex bending, concave bending, and stretching. Frictional effects are seen as areas of surface galling, where the zinc surface is smeared, as in the large concave bend on the lower portion of this section

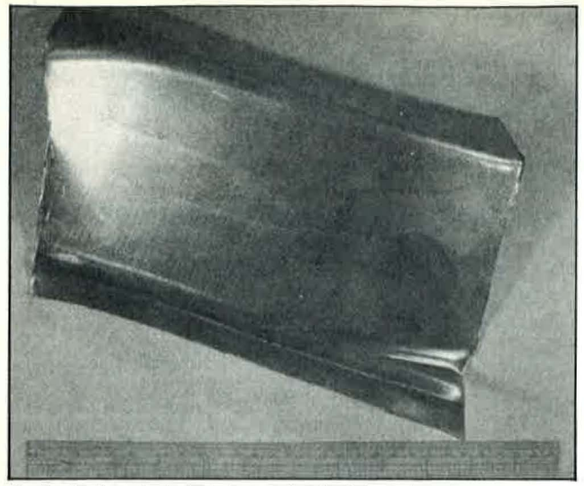

Fig. 5—Section of a typical electrogalvanized sheet stamping.

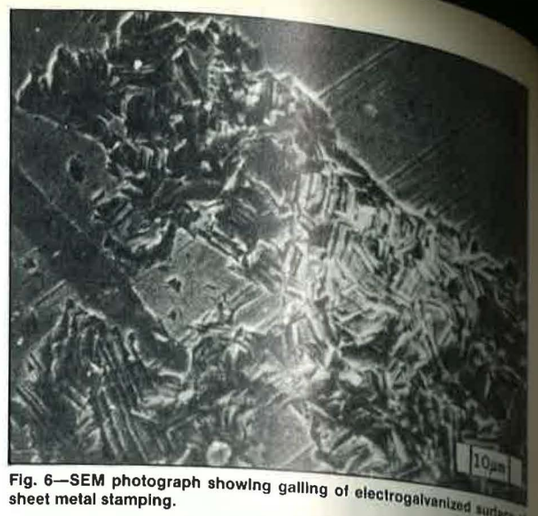

Fig. 6—SEM photograph showing galling of electrogalvanized surface of sheet metal stamping.

(Fig. 6). The net result is to alter the deposit structure.

We prepared deposits that approached the extremes of total basal and total prism plane alignment. Basal-oriented deposits were successfully produced. Low-index pyramid-oriented deposits, with steeply tilted basal planes, were as close to the ideal of prism plane orientation as could be produced. Three types of commercial samples were also studied. The deposit structure and surface morphology were examined and related to forming properties.

Experimental Procedure

Zinc deposits were produced in a polypropylene flow cell, moving the electrolyte past stationary parallel electrodes to simulate a strip line. The cell, designed for one-side deposition, is shown in Fig. 7. The anode consisted of lead with 1.0 weight percent silver. Both electrodes were 10 × 20 cm in size, with an electrode spacing of 9 mm. The flow rate was regulated using a bypass loop. Current was supplied from a constant current power supply. Time and current were regulated to produce coating thicknesses of 14 μm (100 g/m^2).

Drawing quality, aluminum-killed (DQAK) sheet steel was used as the basis metal. Residual oil was wiped from the sheet, after which the surface was degreased in trichloroethylene, pickled in 25 percent HCl, anodically electrocleaned, and activated in 10 percent H_2SO_4. After mounting the specimen in the cell, solution flow was begun and the sample was electrogalvanized.

Earlier work[6] showed that orientation depended on temperature, pH, flow rate and current density. At proper values of the variables, one could produce zinc deposits that were primarily oriented with the basal (0001) or pyramid (10$\bar{1}$X) planes parallel with the substrate. Screening tests were run to obtain the optimum conditions for the two deposit types. X-ray diffractometer traces were used to determine orientation. Results are shown in Table 1. The

Table 1
Zinc Orientations Under Selected Deposition Conditions

Process variable				Estimated percent orientation		
Current density, A/dm^2	Flow, m/sec	Temp., °C	pH	Basal (0001)	Prism (10$\bar{1}$0)	Pyramidal (10$\bar{1}$X)
50	2.2	33	3.5	>56	0	35[c]
50	4.2	26	3.5	>60	0	32[c]
150	4.2	26	3.5	>55	0	40[c]
150	2.2	50	3.0	80-95	0	5-20[a,c]
50	2.2	26	4.5	20	0	>75[c]
150	2.2	26	4.5	6	2	80[c]
150	4.2	26	4.5	2	0	80[b,c]
50	2.2	50	4.2	>40	0	>50[c]
150	2.2	50	4.2	>45	0	>45[c]
50	4.2	50	4.2	>40	0	>50[c]
150	4.2	50	4.2	>45	0	45[c]

[a]High-index planes (10$\bar{1}$3), (10$\bar{1}$4) predominant.
[b]Low-Index planes (10$\bar{1}$1), (10$\bar{1}$2) predominant.
[c]Pyramid planes evenly distributed.
[d]Condition selected for study.

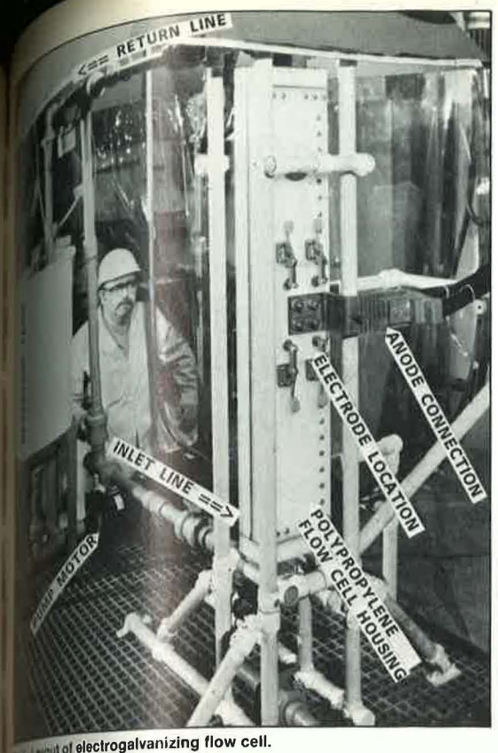

Fig. 7—Layout of electrogalvanizing flow cell.

most strongly influenced orientation. Temperature affected orientation to a lesser extent. The effect of flow rate was negligible.

The optimum conditions for the sulfate plating bath are summarized in Table 2. As the samples were produced, X-ray diffractometry was used periodically to assure reproducibility.

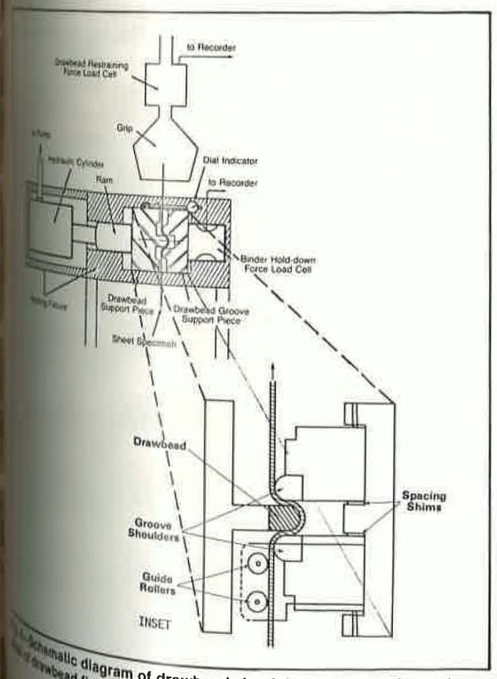

Fig. 8—Schematic diagram of drawbead simulator apparatus. Inset shows detail of drawbead fixture.

The surface morphology of as-plated and deformed deposits was examined by scanning electron microscopy (SEM). Orientation was determined by X-ray diffraction.[10] The percent orientation was estimated by dividing the total corrected intensity count for a given plane by the total corrected count for all planes and multiplying by 100.

A deep draw cup formability test was used to observe changes in surface morphology by deformation. Samples were drawn on an Olsen sheet metal tester. The zinc-coated side was covered with a thin sheet of polyethylene to serve as a lubricant and eliminate galling for clearer study. The sample was drawn into a cup (33 mm deep by 42 mm in diameter), which was then examined in areas representing different modes of deformation.

Drawbead simulation testing was used to determine the friction characteristics of the electrogalvanized steel. The apparatus, shown in Fig. 8, was used in a universal testing machine. A specimen (5 cm wide by 20 cm long) was drawn through a set of three fixed drawbeads, which duplicated the drawbead geometry (Fig. 1 inset). A hydraulic ram maintained the clamping force, while the strip was drawn through the fixture (Fig. 8 inset). Load cells measured the clamping and drawing loads.

It was noted earlier that the drawbead force consisted of friction and deformation components. When pulling through the fixed beads, the combined force was measured. In order to determine the component forces, a roller bead fixture was used in which the fixed beads were replaced by free-rolling cylinders. Assuming negligible rolling friction, the force measured with this fixture was solely due to deformation.

The coefficient of friction is the ratio of friction stress, τ, to normal stress, P, or:

$$\mu = \frac{\tau}{P} = \frac{\frac{D_{d+f}}{A} - \frac{D_d}{A}}{2 \cdot \frac{\pi}{2} \cdot \frac{C_{d+f}}{A}} = \frac{D_{d+f} - D_d}{\pi C_{d+f}} \qquad (1)$$

where D_{d+f} = measured drawing force for fixed drawbeads; D_d = measured drawing force for "frictionless" drawbeads; and C_{d+f} = measured clamping force for fixed drawbeads.

The remaining terms represent an area factor based on passage of the strip around two half-circumferences of a drawbead surface. Comprehensive discussion of drawbead simulation methods is given elsewhere.[1,2]

The development of drawbead tests was based on friction forces acting on both sides of the strip. For steel coated on one side, as in this work, the test was modified to provide friction forces only on the plated side and roller

Table 2
Optimum Plating Conditions for Oriented Deposits

Condition	Orientation: Basal	Orientation: Low-index pyramidal
Zinc metal, g/L	100	100
Current density, A/dm^2	150	150
Temperature, °C	50	30
Flow velocity, m/sec	2.2	4.2
pH	3.0	4.5

action on the bare side. The right side of the fixed bead fixture shown in the inset of Fig. 8 was replaced with the corresponding side of the roller bead fixture. Since the strip would contact the drawbead over one-half circumference, the coefficient of friction would be:

$$\mu = \frac{\tau}{P} = \frac{\frac{D_{d+f}}{A} - \frac{D_d}{A}}{\frac{\pi}{2} \cdot \frac{C_{d+f}}{A}} = 2 \cdot \frac{D_{d+f} - D_d}{\pi C_{d+f}} \qquad (2)$$

Although the commercial samples were coated on two sides, the same one-side friction test was used to maintain a common frame of reference.

Two lubricants were used in the drawbead studies: (1) a split-phase prelube oil to simulate actual drawing conditions, and (2) a thinner mil oil to test under adverse drawing conditions. The surface morphology of the drawbead-tested specimens was examined with the SEM to observe changes, if any, in the deposit.

Results and Discussion

The surface morphologies of the as-plated zinc deposits are shown in Fig. 9. The crystal orientation data is given in Table 3. The basal deposits differed markedly from the pyramidal ones, which resembled commercial deposit surfaces. The commercial deposits, while similar, showed variation in basal plane tilt and grain size.

When conditions favored basal plane alignment, the morphology changed drastically (Fig. 9a). The vertical stacking allowed a more open structure between grains. X-ray diffractometry showed the dominance of the basal plane reflections. Virtually all other planes were absent.

The pyramid plane surface (Fig. 9b) resembled the surface of a commercial deposit (Figs. 9c-e). In fact, Group C samples showed X-ray spectra similar to that for low-index pyramid deposits from the flow cell. The flow cell deposit, however, had a larger and more variable grain size.

The flow cell results confirmed that electrolytic and hydrodynamic conditions influenced the structure and morphology of the zinc electrodeposits. Electrolyte pH was dominant in influencing the orientation of the basal planes.

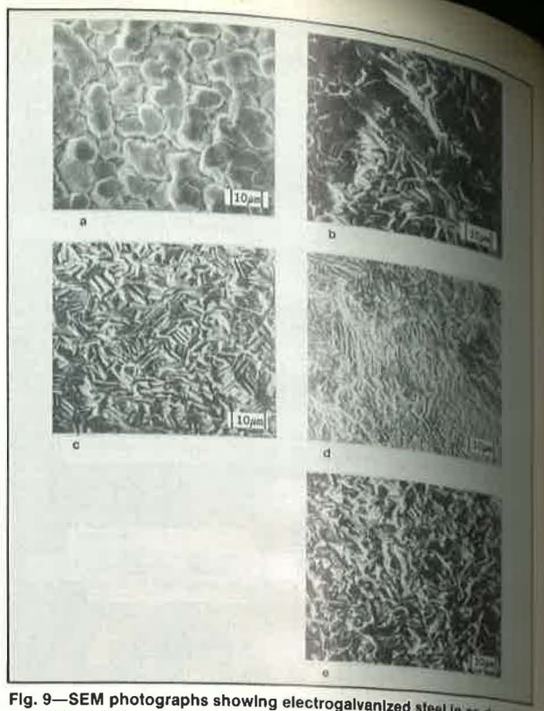

Fig. 9—SEM photographs showing electrogalvanized steel in as-deposited condition: (a) basal plane deposit; (b) pyramidal plane deposit; (c) commercial deposit "A"; (d) commercial deposit "B"; and (e) commercial deposit "C".

The surfaces of the basal and pyramid specimens showed significant differences in deformation behavior. The SEM results are shown in Figs. 10 and 11 for the basal and pyramid deposits, respectively. The draw cup surface underwent various deformation modes, depending on location. The primary deformation characteristic of the basal-oriented deposit was elongation. The slip effect hypothesized in Fig. 4 is evident in Fig. 10. In the area of draw deformation, (a), the zinc grains were elongated, but

Table 3
X-Ray Diffractometer Results
Orientations

	Estimated percent orientation, sample				
Plane	**Basal**	**Pyramidal**	**"A"**	**"B"**	**"C"**
Basal					
(0001)	99.2	5.8	3.9	59.6	5.8
(0002)	0.2			0.1	
Σ	99.4	5.8	3.9	59.7	5.8
Pyramid					
(10$\bar{1}$1)		62.9	21.6	12.8	69.1
(10$\bar{1}$2)		11.3	24.0	4.9	11.3
(10$\bar{1}$3)	0.6	13.5	45.5	21.4	8.8
(11$\bar{0}$2)		3.2	3.9	0.1	4.0
Σ	0.6	90.9	95.0	39.2	93.2
Prism					
(10$\bar{1}$0)		3.0	1.1		0.5
Σ	0.0	3.0	1.1	0.0	0.5

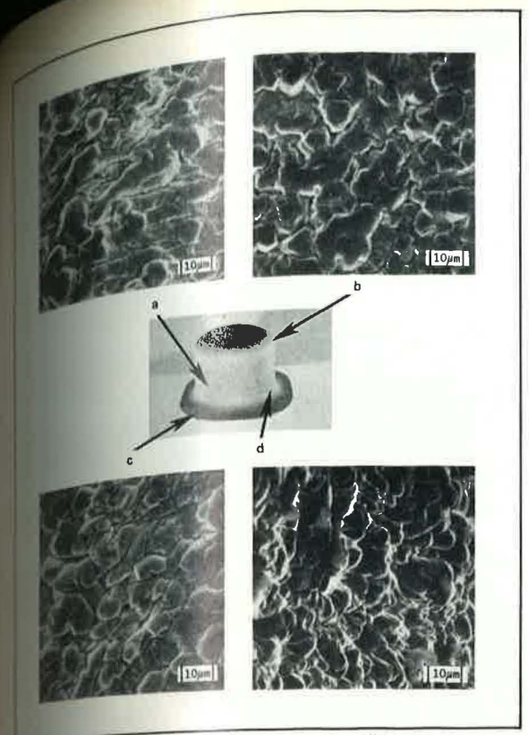

Fig. 10—Draw cup results from basal plane samples: (a) stretch draw area; (b) tensile bend; (c) binder area; and (d) binder flow plus concave radius.

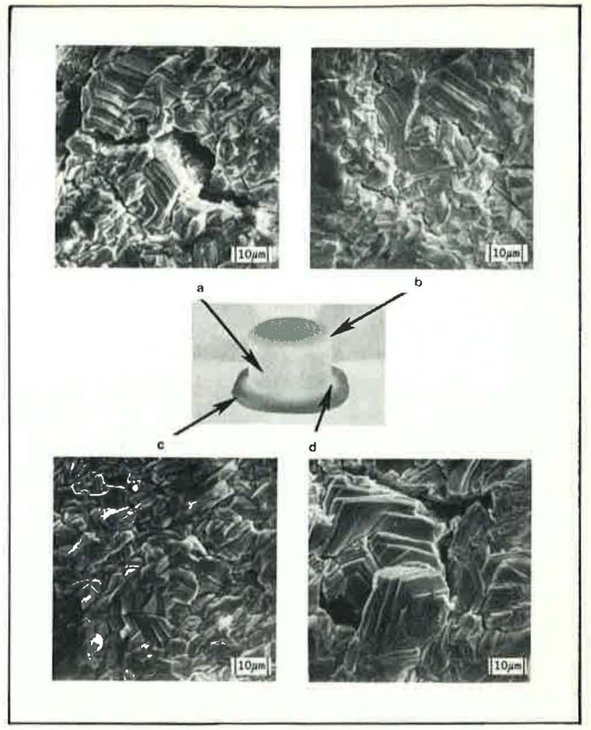

Fig. 11—Draw cup results from pyramidal plane samples. Samples (a), (b), (c), and (d) represent the same areas as in Fig. 10.

no fracture was evident. In the tensile bend, (b), the surface was undisturbed. Some elongation was seen in the binder area, (c). In the concave bend, (d), grain realignment from compressive stress was noted.

Fracture was dominant in the pyramid plane deposits (Fig. 11). This was in line with the cracking suggested in the diagram of Fig. 4. Cracking was dominant in the draw deformation, (a), and tensile bend, (b), areas. The deposit in the binder area, (c), was subject to draw deformation; grain elongation and reorientation were noted. Cracking occurred in the concave radius, (d). The variation in grain size is evident in these photos.

The surfaces of flow cell and commercial deposits after drawbead simulation with and without prelubricant are presented in Figs. 12 and 13, respectively. Both flow cell deposits showed the same characteristics seen in the draw cup study (Fig. 12). Basal plane deposits showed little change, while the low-index pyramid deposits fractured. A pattern of parallel cracks normal to the draw direction is noted at low magnification (200X) (Fig. 12b,d).

All deposits exhibited galling in the drawbead study. This related to the test procedure, rather than to the nature of the deposits. The polyethylene sheet prevented galling in the draw cup study. Galling in drawbead areas is not uncommon in practice. Such areas are designed to be restricted to areas trimmed off the final part in the later stages of the stamping sequence.

The use of the prelube reduced galling for both types of deposits. The galled area was reduced when compared with a specimen run without lubricant. There was little difference between those run with the poor lubricant (mil 20) and those run dry.

The main effect of drawbead deformation on the commercial specimens was galling (Fig. 13). Surprisingly, no

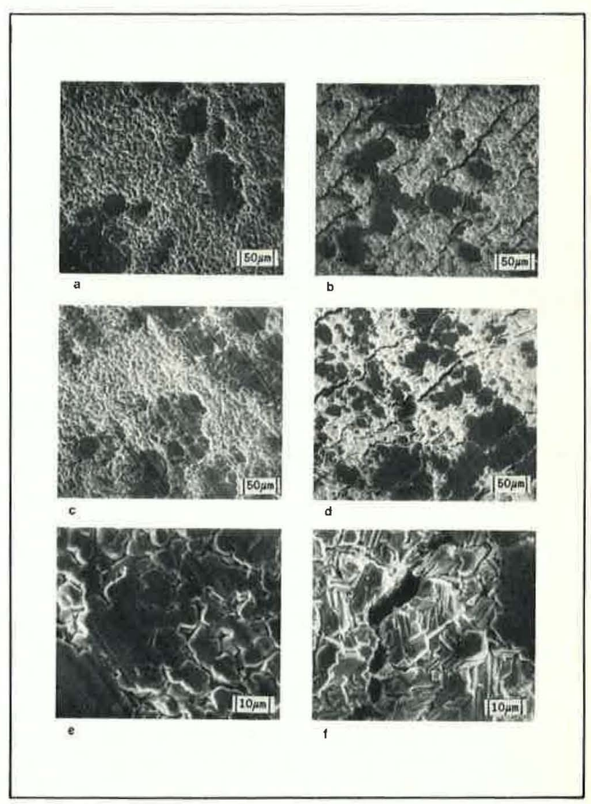

Fig. 12—SEM photographs showing orientation groups of electrogalvanized zinc surfaces after drawbead tests: (a) basal, prelube; (b) pyramidal, prelube; (c) basal, dry; (d) pyramidal, dry. Samples (a) through (d) are low magnification SEMs; (e) and (f) are basal and pyramidal surfaces, respectively, at high magnification.

cracking was found in the Group C deposits, whose orientation was identical to that of the low-index pyramid plane deposits from the flow cell. This difference may be due to grain size, which in turn is determined by deposition conditions. The grain size of the Group C deposits was smaller and more uniform than that of the flow cell deposits.

Coefficient of friction results are shown in Table 4. With the prelubricant, the results vary little from one group to another. The lubricant is doing what it is supposed to do. With poor lubrication, differences become apparent.

For the mil oil tests, the basal deposits showed higher friction than the pyramid ones. This alignment, in aggregate, gave rise to an increase in surface contact area, as in Fig. 14a. The pyramid and commercial deposits would have reduced contact area, with the point- or line-type contact shown in Fig. 14b. These effects were also observed qualitatively. Galling accumulated zinc on the drawbead. The buildup was greater with basal deposits, which exhibited higher friction.

The friction for the pyramid plane specimens was lower than that for the commercial samples. Since these samples had identical orientation, reasons for this difference are not clear. It may be because the commercial samples were electrogalvanized on both sides. Also, the combination roller bead/fixed bead fixture could have subtly changed the pull characteristics of the test. Zinc buildup may also have contributed.

Forming characteristics of electrogalvanized sheet steel can be altered by varying the structure and surface of the zinc electrodeposit. The low-index pyramid structures cracked during deformation. Fortunately, the commercial deposits did not crack. However, because of the profound effect of pH on structure, the importance of process control is apparent.

The results of this work would lead one to expect that the interactions between orientation and forming properties could carry over to other properties, including phosphatability, paintability, and durability. Wang,[11] in a study of the corrosion of single zinc crystals, found that various crystallographic planes will corrode at different rates. The basal plane exhibited the slowest rate. It may be that the orientation can affect corrosion and, because of surface reactivity, the phosphating process. Future work will address these issues.

Conclusions

1. In sulfate electrogalvanizing baths, variations in electrolyte pH will have a major influence on the zinc orientation and surface morphology.

2. Zinc electrodeposits (prepared in the laboratory from a sulfate bath), in which the basal planes are oriented parallel to the substrate surface, undergo elongation in draw deformation. The distortion was not detrimental to coating integrity.

3. Zinc electrodeposits (prepared in the laboratory from a sulfate bath), in which the pyramid planes are oriented parallel to the substrate surface, can undergo fracture in draw deformation and bending.

4. Commercial zinc deposits (from sulfate baths), in which the pyramid planes are oriented parallel to the substrate surface, retained integrity under draw deformation and bending. The difference in performance with the laboratory deposits may be related to grain size effects.

5. The coefficient of friction of basal plane deposits is higher than that for pyramid plane deposits, owing to geometric surface area factors. This difference is erased with an efficient lubricant.

Table 4
Drawbead Test Results
Coefficient of Friction

Sample	Coefficient of friction, oil	
	Prelube	Mil oil
Basal	0.11	0.19
Pyramidal	0.11	0.13
"A"	0.09	0.14
"B"	0.11	0.16
"C"	0.10	0.16

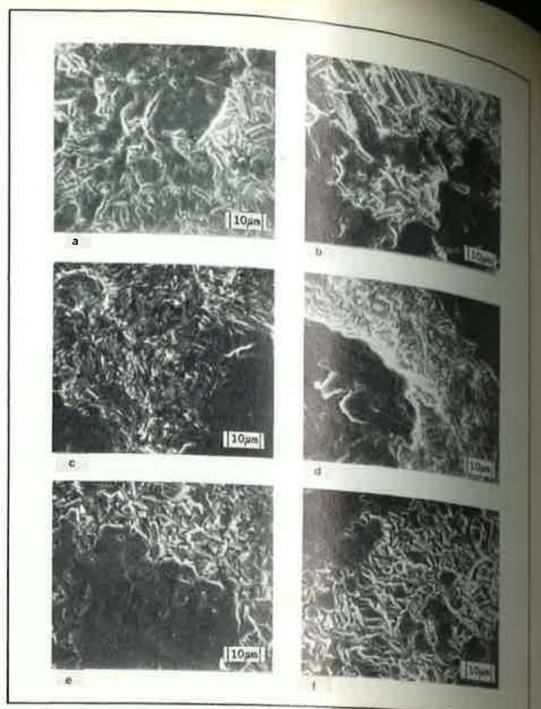

Fig. 13—SEM photographs showing commercial samples of electrogalvanized zinc surfaces after drawbead tests: (a) sample "A", prelube; (b) sample "A", mil oil lubrication; (c) sample "B", prelube; (d) sample "B", mil oil; (e) sample "C", prelube; (f) sample "C", mil oil.

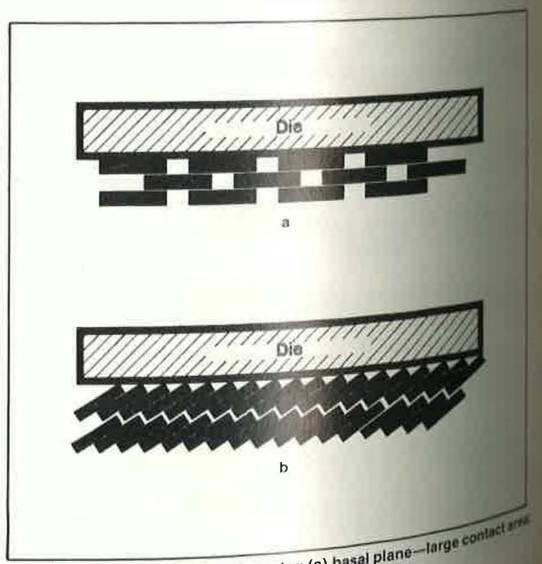

Fig. 14—Die/deposit contact geometry: (a) basal plane—large contact area; (b) pyramid plane—reduced line and point contact area.

Acknowledgments

We are indebted to R. Prater Jr., T. Stachowski, J. Muehorter and J. Laverty of the Rolla Research Center (U.S. Bureau of Mines) for preparing the flow cell deposits. The efforts of R.S. Conell, GM Research, and H.M. Wang, University of Missouri—Rolla, in performing the X-ray diffraction work, and the assistance and helpful comments of Mr. J.J. Moleski, GM Research, in the drawbead work are also appreciated. Finally, we are indebted to J. Bronson, C.P.C. Group Engineering, for providing the commercial material.

References

1. Harmon D. Nine, *Mechanics of Sheet Metal Forming*, D.P. Koistinen and N.-M. Wang, eds., Plenum Press, New York, NY, 1978; p. 179-211.
2. H.D. Nine, *J. Applied Metalworking*, **2**(3), 200 (1982).
3. D.J. Meuleman and J.J. Zoldak, *SAE Technical Paper No. 860432*, SAE, Warrendale, PA (1986).
4. S.P. Keeler and T.E. Dwyer, *SAE Technical Paper No. 860433*, SAE, Warrendale, PA (1986).
5. W.G. Brazier and R.W. Thompson, *SAE Technical Paper No. 860434*, SAE, Warrendale, PA (1986).
6. S.F. Chen et al., *Proc. AESF 5th Continuous Plating Symposium* (1987).
7. T.R. Roberts and F.H. Guzzetta, ibid.
8. V. Jiricny, H. Choi and J.W. Evans, *J. Applied Electrochem.*, **17**, 91 (1987).
9. D. Hull, *Introduction to Dislocations*, Pergamon Press, New York, NY, 1965.
10. B.D. Cullity, *Elements of X-ray Diffraction*, Addison-Wesley, Reading, MA, 1959.
11. Y.-M.Wang, private communication (1987).


Lindsay


Paluch


Nine


Miller


O'Keefe

About the Authors

Dr. James H. Lindsay is a staff research engineer in the Physical Chemistry Dept., General Motors Research Laboratories (GMRL), Warren, MI 48090-9055. He holds BS and MS degrees, respectively, in mechanical and metallurgical engineering and received his PhD in metallurgy from Penn State University. Dr. Lindsay is a member of the Continuous Steel Strip Plating Committee and is vice chairman of the AESF Research Board.

Robert F. Paluch joined GMRL in 1971 and has been involved in electrochemical surface processes, including electrogalvanized and protective coating research. He was employed in the steel casting industry before joining General Motors.

Harmon D. Nine is a senior staff scientist in the Physics Department of the GMRL. He received his BS and MS degrees in physics from the University of Michigan. His current research interests include friction and lubrication in sheet metal forming. Mr. Nine is the author of approximately 30 technical papers.

Vernon R. Miller is a group supervisor in the Resource Processing Division of the U.S. Bureau of Mines, Rolla Research Center, Rolla, MO 65401. He received his BS degree in physics from Kansas State University, with advanced studies at the Oak Ridge Institute of Nuclear Studies and the University of Missouri—Rolla. Mr. Miller has 29 years' experience in metallurgy research, including radioisotopes in steel, soldering and brazing of metals, detectors for ore sorting, recovery of metal values from smelter wastes, and electrogalvanizing.

Dr. T.J. O'Keefe is a professor of metallurgical engineering and Senior Investigator MRC at the University of Missouri—Rolla. His current areas of research and teaching are related to electrodeposition and corrosion processes, as well as other areas of chemical metallurgy.